A hippocampal model for behavioral time acquisition and fast bidirectional replay of spatio-temporal memory sequences

Marcelo Matheus Gauy[1,*], Johannes Lengler[1], Hafsteinn Einarsson[1]
Florian Meier[1], Felix Weissenberger[1], Mehmet Fatih Yanik[2], Angelika Steger[1]

June 11, 2018

[1] Department of Computer Science, Institute of Theoretical Computer Science, ETH Zurich, Zürich, Switzerland.
[2] Department of Information Technology and Electrical Engineering, Institute for Neuroinformatics, ETH Zurich, Zürich, Switzerland.
[*] Contact information: marcelo.matheus@inf.ethz.ch

Abstract

Fast bidirectional replays of place cell activity reflecting previous paths, and stripped off any instantial specifics of the animal's locomotion such as its speed or the duration of stops, have been observed during rest in rodents. Mechanisms underlying replays are not fully understood, as previous models depend on assumptions about the path, and on instantial specifics of motion. Relying on sharp-wave events, dendritic spikes and cholinergic modulation, we propose a spiking network model that stores traversed paths on a behavioral timescale with single exposure and produces fast bidirectional replays of corresponding place cell sequences independent of instantial specifics and the path taken. With the model, we make an experimentally verifiable prediction, the sequence cell population, whose firing follows a predefined sequential activity pattern independent of the environment. Furthermore, we hypothesize a functional role for disinhibition as behavioral time pacemaker, enforcing progression of sequence cell activity to match place sequences traversed.

1 Introduction

An animal's ability to acquire and retrieve episodic memories is essential to guide its decision making and how it interacts with the environment. The hippocampus carries an important role in episodic memory encoding [1, 2, 3, 4, 5], and in long term memory consolidation processes [6, 7, 8]. During exploration, hippocampal neurons display oscillations in the 5 Hz to 12 Hz frequency range (theta state) [9, 10], which is believed to be important for episodic memory encoding [11]. During rest, the hippocampus exhibits synchronous bursts of activity (sharp-wave ripples) [12, 13, 14], and previously stored memories are replayed on a faster timescale [12, 15, 16], thus, being reinforced (consolidated). These consolidation processes (replays) occurring during sharp-wave ripples are essential in reorganizing and strengthening memory traces [17, 18]. Over time, replays slowly transfer these memory traces to the neocortex [19], where they are likely to have a qualitatively different and compressed representation that factors out unnecessary

specifics of a particular experience. Furthermore, sharp-wave ripples reactivate previously encoded memories after a single instance of an experience, enabling said experience to be consolidated as a memory [15, 20, 21].

Navigation in novel environments is a prime example of a task where the hippocampus is crucial in the development of an internal cognitive map supporting spatial awareness, place representation and the subsequent encoding and consolidation of episodic memories [22, 2, 23]. Hippocampal place cells are known to fire at specific spatial locations in a given environment [24, 22, 25]. An animal which navigates in an environment, will do so varying particular *instantial* specifics of its motion, such as its speed, the stopping locations and the duration of these stops. These instantial specifics will, in turn, affect place cell firing profiles during the exploratory state, producing behavioral time sequences of place cell activity that depend on such specifics. Still, one observes spontaneous fast forward and reverse replay of this sequential place cell activity in sharp-wave ripples during sleep [15, 20] and quiet wakefulness [26, 27, 21, 28, 29, 30], which are independent of the speed, the stopping times and stopping locations of the animal [15, 31, 32, 33, 28]. The works of [33, 28], in particular, provide strong support for the correlation between the length of replay events and that of the traversed path, suggesting that replays possess nearly constant speed. Moreover, these replays of sequential place cell activity occur after a single traversal of the corresponding path [15, 26, 29], indicating that the animal quickly learned an internal representation of the environment independent of the instantial specifics of its motion.

Sharp-wave ripple like activity patterns have been shown to emerge in models of place cell activity where plasticity rules, like STDP [34, 35], shape the network connectivity. Patterns reminiscent of the observed replays in sharp-wave ripples appear, both in a rate-based setting [36, 37] and in spiking networks [38, 39, 40]. However, it has proven difficult to reproduce the aforementioned compressed representation, which must be acquired on a behavioral timescale, and therefore subject to instantial variations in its encoding procedure, and at the same time alternate to a mode of operation (replays), which is orders of magnitude faster and possess nearly constant speed. Furthermore, it remains unclear how such a compressed representation could be acquired after a single traversal of a path, independent of the geometrical configuration of the environment and of the instantial specifics of the animal's motion. Moreover, using exclusively the recurrent connectivity among place cells to reproduce the phenomena of replays poses a challenge when dealing with loops in the path of the animal (i.e. crossing of paths) that otherwise must be represented/discriminated by different place cell ensembles [41, 42].

In this work, we solve this challenge by presenting a model that can store experienced trajectories on a behavioral timescale, and produce fast bidirectional replays after a single run of the trajectory. Furthermore, no assumptions are necessary on the geometry of the environment and on the specific trajectory taken (such as whether it contains loops). As dealing with trajectories containing loops is difficult using exclusively recurrent connectivity among place cells, our model predicts the existence of a particular functional type of cells, which we term **sequence cells**. Unlike place cells, which fire at a particular location, *sequence cells* fire in a predefined sequence independent of the environment, thus, representing a position in an abstract sequence. In other words, a sequence cell ensemble representing the fourth position in the sequence would always fire at the fourth location the mouse has been through since the sequence has started, independent of which location it actually is. This abstraction allows one to deal with trajectories that contain loops (crossings in the path) and is in principle the easiest approach to the problem, as alternative solutions involve more complex mechanisms to distinguish the internal state of the network between the different moments the crossings in the path took place. Furthermore, sequence cells are an experimentally verifiable (though challenging) hypothesis as they have a pattern of activity clearly distinguishable from place cells and from other specific characteristics

of the movement such as head direction, border, speed and so on (though they could be difficult to distinguish from time cells [43], as in a sense, sequence cells also measure time). Lastly, we observe that morphological and electrophysiological observations reported in the literature indicate a large diversity of CA3 principal cells for both rodents and primates [44, 45]. While the functional roles of these diverse types of CA3 neurons remains unclear, there is a growing belief that this hetereogeneity supports a functional segregation of the information processed in the hippocampus [46].

Our model operates in two distinct modes: an **encoding mode**, corresponding to the hippocampal theta state observed during navigation and a **replay mode**, corresponding to sharp-wave ripples observed during sleep and quiet wakefulness. In the *encoding mode*, the synapses from sequence cells to the corresponding place cells are learned by standard Hebbian plasticity rules. Thereby, the sequence cell ensembles representing positions in the sequence are associated to the place cell ensembles representing locations. These learned associations will enable replays of place cell activities. As the time spent on each location is irregular during navigation, the progression of sequence cell activity in the abstract sequence is controlled by disinhibition. Disinhibition effectively signals that a new location has been reached, which induces the next ensemble in the sequence to turn active. This novelty signal, therefore, enforces simultaneous progression in the abstract sequence represented by sequence cell activity and the sequence of locations visited represented by place cell activity. Consistent with our postulate of disinhibitory input shaping activity patterns to match behavioral navigation times, it has been reported that glutamatergic interneurons in the medial septum effectively control speed-correlated firing of hippocampal neurons [47, 48]. The *replay mode*, unlike the encoding mode, exhibits extremely synchronous activity as observed in sharp-wave ripples [12, 14]. This synchrony of activity induces dendritic spikes, which produce a fast forward and/or reverse replay of the sequence cells. The replay of sequence cells in turn produces forward and/or reverse replay of the place cell ensembles in the order the connections from the sequence cell ensembles to the place cell ensembles are learned. Consistent with previous theoretical work [38] and experimental observations [49, 14], our model proposes that replays, dendritic spikes, sharp-wave ripples and cholinergic modulation are tightly interconnected. In fact, septal cholinergic activation to CA3 pyramidal neurons has been experimentally shown to enhance theta oscillations and effectively suppress sharp-wave ripples in the CA3 network [49, 50, 51]. The nicotinic receptors either on the soma, pre-synaptic boutons, or post-synaptic spines of CA3 pyramidal cells can effectively inhibit firing of CA3 pyramidal neurons. Another potential inhibitory mechanism could be through the GABA-B receptors on CA3 pyramidal neurons, which can serve a similar role, although the origin of inputs to GABA-B receptors are currently unknown.

We simulate a spiking network of exponential integrate-and-fire neurons with physiological parameters to show that a sequence cell population, with disinhibitory input as behavioral time pacemaker during encoding (theta state) and dendritic spikes and cholinergic modulation as the network mechanism of inducing synchronous bursts in the replay mode (sharp-wave ripples), can fully reproduce the phenomena of replays, by simulating a spiking network of exponential integrate-and-fire neurons with physiological parameters.

2 Results

2.1 Encoding of place cell sequential activity

We demonstrate that the hypothesis of a sequence cell population can account for the robust forward and reverse replays observed in the hippocampus. This is done through the simulation

of a virtual mouse exploring a predefined environment. A spiking neural network of exponential integrate-and-fire neurons with physiological parameters, emulating the behavior of place and sequence cells, is associated to the mouse. We produced a video animation (link) to enhance the comprehension of what the model achieves and of how it does so.

As the mouse walks through the environment, a sequence of place cells in the spiking neural network will fire, each place cell corresponding to a particular place in the environment[1]. In parallel, the sequence cells of the spiking neural network also fire, but they do so along a predefined sequential activity pattern, which is independent of the environment and the route taken by the mouse. Crucially, after exploration of the environment by the mouse, the sequence cell activity is capable of triggering replays of place cell activity, due to the plasticity of synapses between sequence and place cells. These sequence cells can be used to replay many different sequences of place cell activity. We defer the detailed explanation of the mechanism that allows sequence cells to produce the desired behavior to the next subsection. For ease of understanding we first provide some general intuition relating sequence cell dynamics to the place cell activity.

Consider as an example, a virtual mouse walking on a track, as depicted in Figure 1A. Each place cell corresponds to a specific location on the track. The place cells fire with $\approx$50 Hz when the mouse is at the corresponding location, and are otherwise silent. As the mouse moves along the track, a sequence of place cell ensembles is activated. The place cells are also targeted by sequence cells and plastic synaptic connections will encode the sequence of place cell activity produced by the motion of the mouse, as shown in Figure 1B. The sequence cells fire following a predefined activation pattern that possesses two modes of operation: the **encoding mode** and the **replay mode**. These correspond to the experimentally observed different modes of operation at the hippocampus during exploration and slow-wave sleep (or quiet wakefulness), respectively. In the *encoding mode*, the next ensemble in the sequence is only activated when the mouse moves to another location. The synapses from sequence cells to the corresponding place cells are learned and, thereafter, sequence cells can activate the corresponding place cell ensembles without requiring external input from the environment, as illustrated in Figure 1C. The applied learning rule is a simple Hebbian plasticity mechanism (a detailed description of the applied learning rule is given in the Materials and Methods section).

Thus, in the encoding mode, the place cell ensembles are activated in sequence as the animal moves along the track, as shown in Figure 1D. In the *replay mode*, the sequence cell ensembles are triggered one after the other, in a small time window. Through the synaptic connections that were learned in the encoding mode, the sequence cells trigger a forward replay of the place cells. A raster plot of place cell activity during the replay mode is shown in Figure 1E. Furthermore, the sequence cell ensembles can also be activated in the opposite order, and this produces reverse replay of place cell activities. A raster plot of a reverse replay of place cell activity is shown in Figure 1F. It may be noted that both forward and reverse replay are much faster than the original encoding time, that they are independent of the animal's speed, stopping times and locations, and that the majority of place cells fire in the right order, driven by the activity of the sequence cells. Moreover, these replays can be produced after a single traversal of the path by the mouse.

We emphasize that our approach does not require any particular assumption on the geometry of the environment, the connectivity among the place cells and particularities of the path (such as loops). Sequence cells enable our model to produce replays in such a general setting, and this is discussed in the next subsection.

[1]In the model, we do not speculate how place cells could correspond to a particular place in an environment. Instead, when the mouse is at a certain location, we enforce that the corresponding place cell ensemble fires at the correct rate, as is experimentally observed [22].

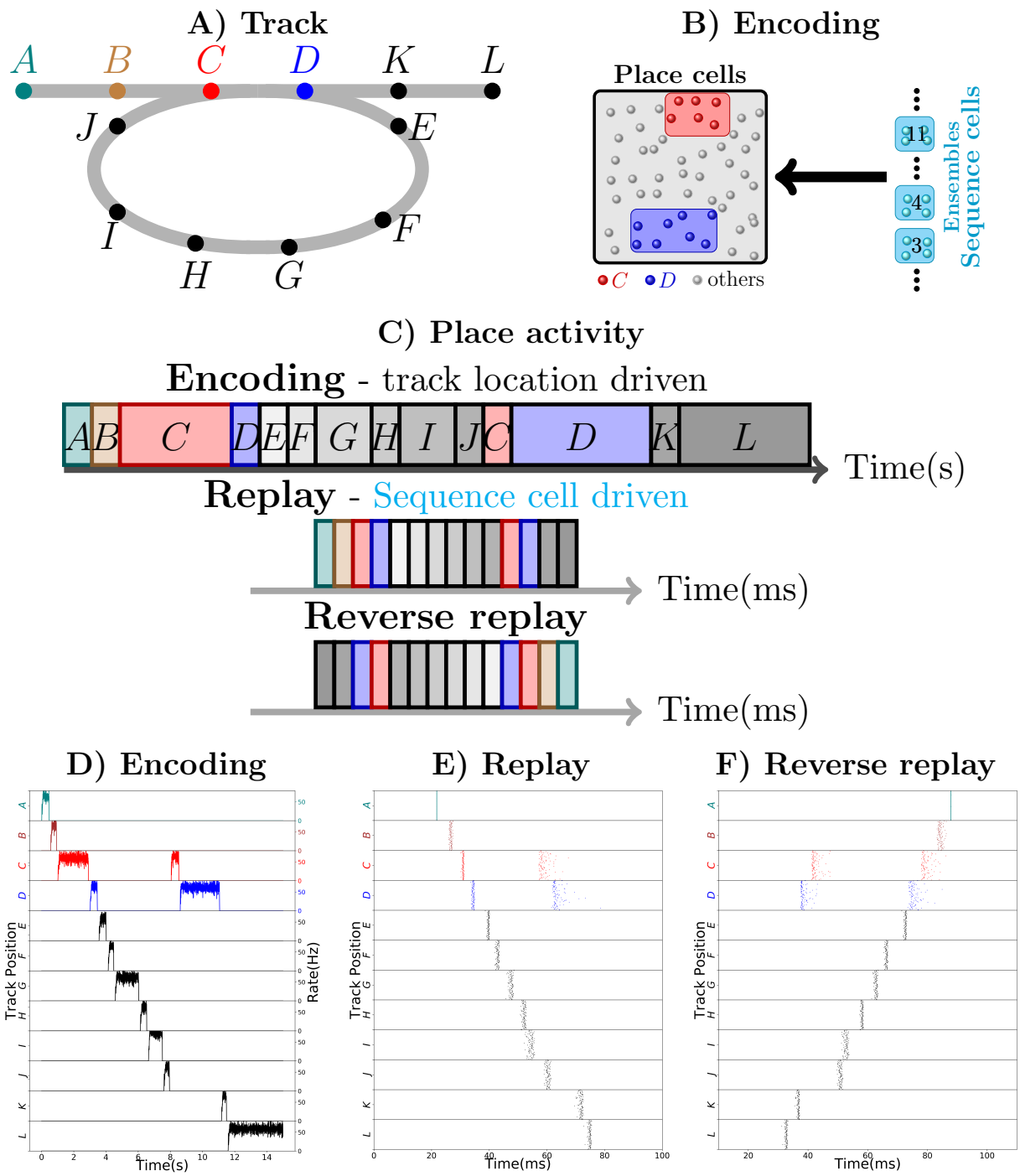
A) Track
A
B
C
D
K
L
J
E
I
F
H
G
B) Encoding
Place cells
C
D
others
11
4
3
Ensembles
Sequence cells
C) Place activity
Encoding - track location driven
A B C D E F G H I J C D K L
Time(s)
Replay - Sequence cell driven
Time(ms)
Reverse replay
Time(ms)
D) Encoding
E) Replay
F) Reverse replay
Track Position
Rate(Hz)
Time(s)
Time(ms)

Figure 1

Figure 1 *(previous page)*: Robust replay of place cell activity. (A) An animal walks along a path, containing a loop in a 2-dimensional environment. (B) Locations in this path are associated to specific populations of CA3 place cells which fire at high rates if the animal is at said location. In this particular scenario, each position is associated with an ensemble of 100 place cells. Concomitantly, the sequence cells fire following a predefined sequential activity pattern that is explained in detail in Section 2.2. Hebbian-like synaptic plasticity connects the sequence cells to the corresponding place cell ensembles. (C) The sequence cell dynamics allow for place cell activity replay on a much shorter timescale and independent of the animal's stopping times and locations. (D) 15 seconds simulation of place cell activity as the animal walks through the track in (A); a rate plot of the place cell ensembles corresponding to each position the animal walks through is shown; the x axis shows time in seconds, the left y axis shows the track positions corresponding to the place cell populations and the right y axis shows the firing rate of each place cell ensemble corresponding to a particular track position. Note that in addition to the loop in the path, the animal occasionally stays arbitrarily longer at particular locations. (E) Fast replay of the path taken by the animal in less than 100ms; a raster plot of place cell activity is shown; the x axis shows time in milliseconds, the left y axis shows the track positions corresponding to the place cell populations. (F) Reverse replay of the path taken by the animal; a raster plot of place cell is shown; the axis are the same as in (E). Note that each weight in the spiking network is multiplied by a gaussian multiplicative noise.

2.2 Sequence encoding modules of sequence cells

Sequence cells are organized in a specific manner that allows them to produce the phenomena of replays observed in place cells in Figure 1. Sequence cells might coexist in the CA3 with the place cells (or might be localized somewhere else in the hippocampus). Figure 2A shows the general structure of sequence cell connectivity, showing an example of what we term a **sequence encoding module**. The sequence cells can, in principle, compose many such modules that could store many parallel sequences. Each sequence encoding module consists of ℓ ensembles of neurons $B_1, \ldots, B_\ell$. Forward connections from B_i to B_{i+1} are present. Backward connections, which allow reverse replays, are also present and are generally weaker than the forward connections. These ensembles share two different sources of inhibition: the **gating** inhibition I_G and the **competitive** inhibition I_C. The rate dynamics of individual ensembles B_i have two stable fixed points, one at low firing rate ($\approx$0 Hz) and one at high firing rate ($\approx$50 Hz). Henceforth, we term the ensembles B_i **bistable units**, and refer to B_i as *active* at a particular time if its instantaneous rate is at the 50 Hz stable point, and *inactive* if it is at the silent stable point. Furthermore, the gating inhibition I_G is also either *active* (if its inhibitory neurons fire at a high rate) or *inactive* (if its inhibitory neurons are silent)

As noted in the previous subsection, these sequence encoding modules possess two modes of operation: the encoding mode and the replay mode. In the encoding mode, only one bistable unit is active at a particular point in time, and this bistable unit remains active for as long as necessary, only triggering activity in the next bistable unit and turning itself inactive when the mouse moves to another location. In the replay mode, the bistable units are triggered one after the other in a very brief period of time.

The discussion of the dynamics of sequence cells is split between this subsection and the subsection **Sequence encoding modules - spiking network**. This is done to distinguish the essential building blocks of our model, presented in this subsection, from specific implementation decisions that are not essential.

2.2.1 Encoding mode

The encoding mode of the sequence encoding modules relies on a specific, complex rate dynamics while the animal is exploring an environment. To describe them, and to extract the fundamental ingredients that allow a spiking neural network to produce the desired behavior, we first adopt a **mean-field approach** and collapse the bistable units B_i, the gating inhibition I_G and the competitive inhibition I_C into abstract rate units. This approach is inspired by [52, 53]. A detailed description of this rate-based system is given in the Materials and Methods section.

At all times, the *competitive* inhibition I_C guarantees that only one bistable unit B_i can be active at any particular point in time, by realizing essentially a winner-takes-all mechanism. The *gating* inhibition I_G is responsible for controlling the amount of time B_i remains active. While I_G is active, the currently active bistable unit remains active. If the mouse location changes, I_G turns inactive, which implements a disinhibitory mechanism that allows progression of activity in the bistable units as follows (see the **Discussion** section for experimental evidence relating disinhibition and behavior). As soon as I_G turns inactive, the active bistable unit B_i drives the rate of the inactive bistable unit B_{i+1}. Eventually B_{i+1} turns active and triggers the competitive inhibition I_C. As B_{i+1} receives more input than any other bistable unit (if we set the connections from B_i to B_{i+1} stronger than the ones from B_{i+1} to B_i), it will be the only one active at the end due to the winner-take-all dynamics imposed by I_C. Once B_{i+1} has taken over, the disinhibitory signal is removed and I_G turns active again and prevents B_{i+1} from activating B_{i+2}. Figure 2B shows this evolution of activity in a rate-based system that reproduces the desired rate dynamics.

Figure 2C illustrates the most notable states of activity the network goes through. In (i) while I_G is active, B_i remains active; (ii) once I_G is inactive; (iii) the rate of B_{i+1} is driven up by B_i; (iv) this, in turn, triggers an increase in the rate of I_C, which (v) forces a competition among B_i and B_{i+1}; eventually, B_{i+1} emerges as the winner and (vi) I_G is again active, preventing B_{i+1} from activating B_{i+2}, while B_{i+1} stays active.

Figures 2D, E show the spiking network of sequence cells transitioning between two consecutive patterns and exhibiting the aforementioned rate dynamics. Note that the length of the period in which the gating inhibition I_G is inactive is different in both. Thus, the length of the period in which the disinhibitory signal is given to I_G does not need to be strictly timed. The most important requirement is that it gives enough time for the dynamics happening between (ii) and (v) to reach its stable point.

Furthermore, as will be seen in the next subsection, when the spiking network obeying these rate dynamics is presented in detail, the encoding mode has two defining characteristics other than the combined gating and competitive inhibitory processing mechanisms. They are: 1) neurons in bistable units fire *asynchronously*; and 2) transition time between one bistable unit and the next is in the order of 50 ms to 100 ms. The first property emerges from a balance of excitation and inhibition in a spiking network of neurons [54, 55] and is crucial in guaranteeing the stable rate dynamics we expect from the bistable units. The latter property is a consequence of having a spiking neural network produce the complex rate dynamics of the sequence encoding modules. Roughly speaking, for the gating inhibition I_G to prevent activation of the next bistable unit, the weights between bistable units must be generally weaker than those inside each bistable unit. Since too high stable rates for a bistable unit B_i are not reasonable, these weights between bistable units units will be weak. Finally, weak weights imply that some time is necessary to increase the membrane potential of the neurons beyond the spiking threshold.

In essence, in the encoding mode, the sequence encoding module activates bistable units in a sequence, with the crucial property that the sequence can be stopped, for an arbitrarily long

period, at any particular point in time. This allows it to capture the essential elements of the path explored by the animal, as the sequence transitions to the next element only when a new location is reached. It may be noted that such an ability to produce compressed representations is potentially useful in other contexts. We discuss further applicability in the Discussion section of the paper.

2.2.2 Replay mode

The main distinguishing feature of the encoding and replay modes is the synchrony of activity. In the replay mode, activity progresses through the bistable units in synchronous waves, reminiscent of a synfire chain [56], in a manner depicted in Figure 3A. This synchrony of activity in a bistable unit yields fast dendritic sodium spikes in the subsequent bistable unit. Dendritic sodium spikes are observed whenever, in a period of a couple milliseconds, the membrane potential at a particular branch of the dendrite of a neuron receives excitatory input above some threshold [57, 58, 59, 60]. Therefore, we assume that the neurons in bistable unit B_i have the axons projecting on close branches of the dendrites of neurons in bistable unit B_{i+1}. We assume a similar structure for the backward connections, as reverse replays will also be driven by dendritic spikes[2]. Whenever B_i is synchronously activated, some branch of the dendritic tree of a neuron in B_{i+1} receives strong excitatory input in a few milliseconds, producing a dendritic spike that has a large depolarizing effect on the soma. Figure 3B shows the effect on the soma of one such dendritic spike, in comparison to the effect that would be produced if dendritic nonlinearities were not present.

There is experimental support for the connection between synchronous events and replays, as replays are observed typically during sharp-wave ripple events, the most synchronous pattern of activity in the brain [63, 64, 14]. In our model, as shown in Figure 3C, the sequence cells can also be played asynchronously forward, without the appearance of dendritic spikes due to the lack of synchrony. In fact, this asynchronous slow replay of sequence cells produces replays that resemble what is experimentally observed during REM sleep [65]. In the model, the forward replays without synchrony are not significantly faster than the original encoding time, with transition between consecutive bistable units is between 50 ms to 100 ms. Such slow transition times are not in line with the speed of forward replays observed during sharp-wave ripples, but they are comparable to the speed of replays observed during REM sleep where sharp-wave ripples are rare and theta activity is predominant [10]. Furthermore, without using synchrony and cholinergic modulation, it is not possible to significantly reduce such transition times. If asynchronous firing of a bistable unit B_i, in a couple of milliseconds, sends too large input to B_{i+1}, then a simple form of inhibitory gating of activity may not prevent B_{i+1} from turning active. Even more, the non-linear effect of dendritic spikes is also crucial if the neurons in B_i are synchronously activated. This is because, without the non-linear effect of dendritic spikes, it is difficult to distinguish high asynchronous firing rates, from synchronous events. Only a couple milliseconds are required for a bistable unit firing at 50 Hz to send forward the same input that it would send if it fired synchronously[3].

Figure 3D shows a fast replay of sequence cells produced by the spiking network. Note that the transition time drops to around 5 ms, that the activity in each bistable unit is very

[2]In the model, we follow the same approach as [61, 62, 38] and assume that given enough synchronous input dendritic spikes will occur.

[3]Lowering the stable rate at which a bistable unit is active would also have undesirable consequences as one needs to be able to clearly distinguish between the low and high firing rate stable points of the bistable units. This will be further discussed in the next subsection.

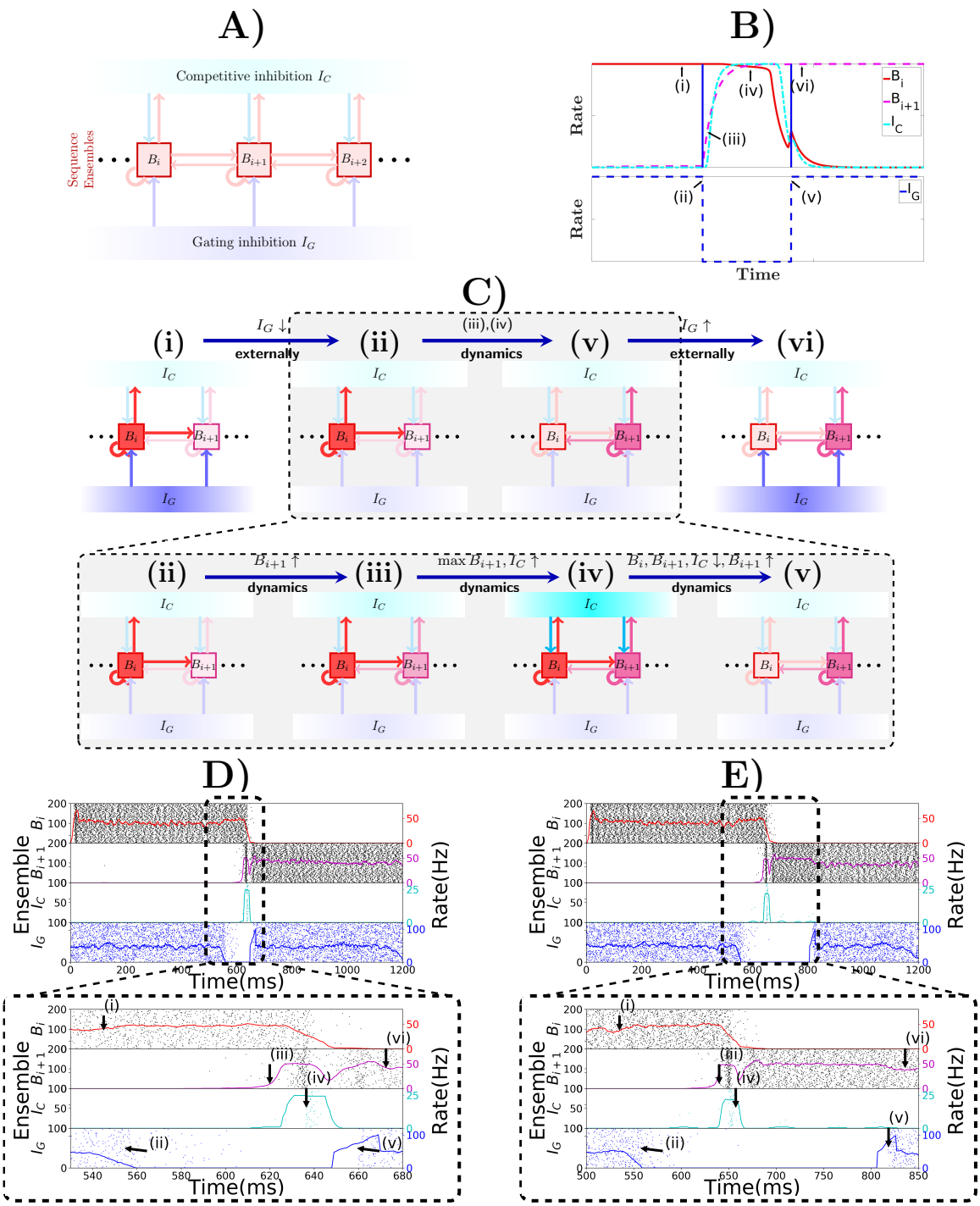
A)
Competitive inhibition I_C
Sequence Ensembles
B_i
B_{i+1}
B_{i+2}
Gating inhibition I_G
B)
Rate
(i)
(iv)
(vi)
(iii)
(ii)
(v)
B_i
B_{i+1}
I_C
I_G
Time
C)
(i)
$I_G \downarrow$
externally
(ii)
(iii),(iv)
dynamics
(v)
$I_G \uparrow$
externally
(vi)
I_C
I_G
B_i
B_{i+1}
(ii)
$B_{i+1} \uparrow$
dynamics
(iii)
$\max B_{i+1}, I_C \uparrow$
dynamics
(iv)
$B_i, B_{i+1}, I_C \downarrow, B_{i+1} \uparrow$
dynamics
(v)
D)
E)
Ensemble
Rate(Hz)
Time(ms)

Figure 2

Figure 2 *(previous page)*: Sequence encoding modules. (A) Illustration of a sequence encoding module architecture consisting of 3 bistable units B_i, B_{i+1}, B_{i+2}, the competitive inhibitory population I_C and the gating inhibitory input I_G. The inhibitory unit I_C prevents two bistable units B_j from having high rate at the same time, whereas the gating inhibition I_G is the "break" that prevents activity from propagating from B_j to B_{j+1}. This break is externally controlled, by some mechanism that recognizes when the animal changes its location. (B) Evolution of the rates of 2 abstract rate units B_i, I_C and I_G, disposed according to the sequence encoding architecture in (A). (C) General illustration of the states the network goes through over time. (i) and (vi) correspond to stable states in the network while I_G is activated. Inactivating I_G induces a dynamical process that brings the network from state (ii) into state (v). This dynamical process is depicted in further detail below with (iii) and (iv). In (iii), due to inactivation of I_G, the activity in B_{i+1} picks up, driven from the activity B_i. As shown in (iv), once both B_i and B_{i+1} are active, they together activate I_C, which gives strong inhibitory input to B_i and B_{i+1} and (in (v)) forces B_i to become inactive, while the recurrent activity permits B_{i+1} to recover and stay active. (D) Spiking network of sequence cells. Above, the x-axis shows 1.2 seconds of simulated activity. The left y-axis shows the indices of the cells in each sequence ensemble, and a raster plot is given. The right y-axis shows the rate of each sequence ensemble. Below, the period where I_G is inactivated is emphasized. During this period, the stability of the system is broken and the dynamics described above take place, leading ultimately to B_{i+1} overtaking B_i as the active sequence ensemble. (E) Analogous to (D), but we now purposedly enforce a longer time out of the global inhibitory mechanism. Observe that the system still functions much like in (D), so the period where I_G is turned off is flexible.

synchronous and that most neurons spike once and in the right order.

The second distinguishing feature between the encoding and replay modes is a different cholinergic environment. In the replay mode, we assume lower levels of Acetylcholine (ACh) in the network. This is motivated by the experimental observation that replays typically occur in sharp-wave ripples during slow-wave sleep and quiet wakefulness, where lower ACh levels are documented [49, 50]. It is known that a lower ACh level makes synapses overall stronger and the network more excitable [66]. In our model, higher excitability is not necessary for forward replays, but it is strictly necessary for reverse replays. Furthermore, higher excitability facilitates faster transition times between bistable units, as well as the occurrence of dendritic spikes. In principle, if there would not be any dendritic spikes, this higher excitability of the network could decrease the transition times between bistable units, even when the bistable units fire in an asynchronous manner. Hence, the higher network excitability would allow for the bistable units to be replayed asynchronously faster than shown in Figure 3C, which would in turn allow for replays even without a synchronous mode containing dendritic spikes. However, in order for the replays to be as fast as what is observed in the literature [20, 64], the magnitude of the cholinergic effect on the network would have to be much higher than what is reported in [66]. Dendrtic spikes are therefore necessary for fast replays of activity, in line with what is reported in the literature.

In short, due to slow transition times, the encoding mode of the sequence encoding module cannot account for the fast robust replays observed in the hippocampus. The module needs another mode of activity that has faster transition times. We remark that this different mode of activity is consistent with biology, as these replays are observed during quiet wakefulness and sleep, where the hippocampus is known to be operating in a different regime. Two essential ob-

served properties of the hippocampus in quiet wakefulness and sleep motivate the replay mode: sharp wave ripples and a different neuromodulatory environment, especially, lower levels of Acetylcholine (ACh). Evidence concerning sharp wave ripples indicate that the sequence encoding module in the replay mode might have its bistable units activated in an almost synchronous manner [14]. Lower ACh levels, as is observed during sleep and quiet wakefulness [49, 50], induce higher excitatory synaptic weights which facilitate faster transitions between bistable units.

2.2.3 Reverse replays

As mentioned before, the reverse replays rely crucially on the higher network excitability produced by lower levels of ACh, whereas forward replays do not. This is because the rate dynamics of the encoding mode lead to a weight asymmetry condition. The backward connections among bistable units that enable reverse replays must necessarily be weaker than the forward connections among bistable units. In particular, this asymmetry gives a potential function for the (experimentally observed) increased excitatory weights induced by lower ACh levels [49, 50]. For the backward connections to produce synchronous activation of the bistable units in reverse order, they need to be strong enough to produce dendritic spikes. However, as they are weaker than the forward connections, in the encoding mode, asynchronous activation of a bistable unit should not produce dendritic spikes in the next one. If the excitatory synaptic weights are not generally increased in the replay mode it is difficult to have, at the same time, dendritic spikes at the backward connections in the replay mode and a fully functioning encoding mode. One either gets instability in the encoding mode, or not enough dendritic spikes in the replay mode. Therefore, reverse replays are made possible by the difference in the neuromodulatory environment, in addition to sharp-wave like synchronous activity triggering dendritic spikes.

Observe, additionally, that dendritic spikes have a refractory period of about 5 ms [61, 62, 38] and that within this refractory period the respective dendrites do not transmit any spikes. It is this refractory period that forces the synchronous wave to travel in a single direction. This is also shown in Figure 3A. In this case, if bistable unit B_i is synchronously activated by dendritic spikes from B_{i-1} (from B_{i+1}), it will produce dendritic spikes only in B_{i+1} (in B_{i-1}), as the neurons of B_{i-1} (of B_{i+1}) are in the refractory period, respectively. Moreover, Figure 3D shows a reverse replay of activity produced by the spiking network.

In essence, the asynchronous encoding mode has a preferred direction for the activity to travel, as the forward connections between bistable units B_i and B_{i+1} are stronger than the backward connections between B_i and B_{i-1}. Dendritic spikes, cholinergic modulation and the refractory period of neurons allow the sequence cells to be activated in both directions, depending on which bistable unit the synchronous volley starts.

2.3 Sequence encoding modules - spiking network

In the previous subsection, the essential building blocks of sequence encoding modules were discussed on a conceptual level. In this subsection, we describe more detailed conditions that are necessary so the dynamical system comprising our spiking network model behaves as intended.

2.3.1 Bistable units

In the spiking network, each bistable unit consists of a recurrently connected population of excitatory and inhibitory cells as depicted in Figure 4A. To produce bistable units where the rate dynamics maintain two stable fixed points, one around 0 Hz and one around 50 Hz, we analyse the gain function [67] of excitatory and inhibitory neurons as shown in the left of Figure 4B.

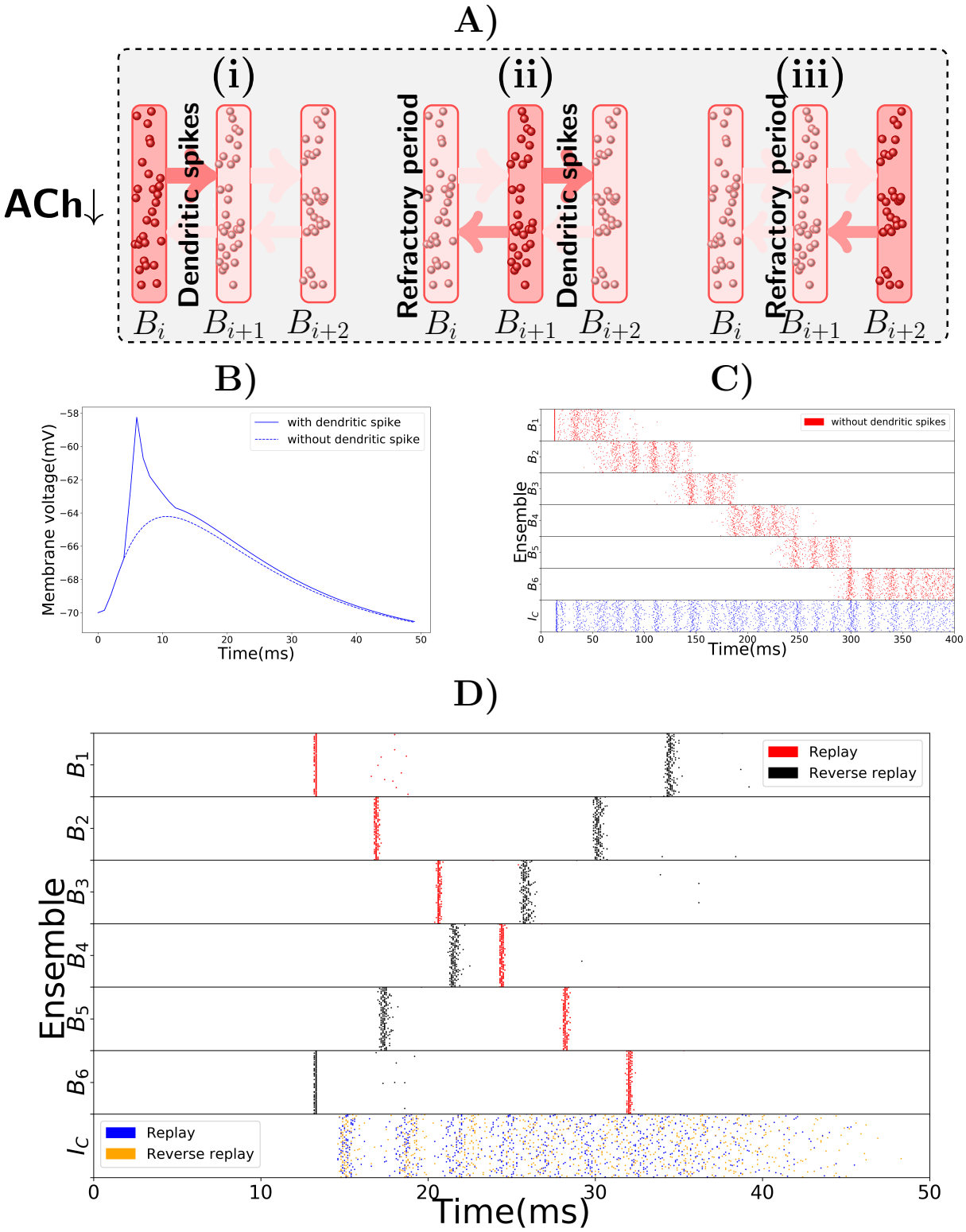
A)
(i)
(ii)
(iii)
ACh↓
Dendritic spikes
Refractory period
Dendritic spikes
Refractory period
B_i B_{i+1} B_{i+2}
B_i B_{i+1} B_{i+2}
B_i B_{i+1} B_{i+2}
B)
Membrane voltage(mV)
with dendritic spike
without dendritic spike
Time(ms)
C)
without dendritic spikes
Ensemble
B_1 B_2 B_3 B_4 B_5 B_6 I_C
Time(ms)
D)
Replay
Reverse replay
Ensemble
B_1 B_2 B_3 B_4 B_5 B_6 I_C
Replay
Reverse replay
Time(ms)

Figure 3

Figure 3 *(previous page)*: Replay mode of the sequence encoding module. (A) Synfire chain like synchronous activation of three consecutive bistable units B_1, B_2, B_3. Synchrony triggers dendritic spikes in the next bistable unit, which in turn synchronously activate it. Activity moves in a single direction due to neurons entering a refractory period. (B) Nonlinear effect of a dendritic spike on the membrane potential at the soma of a neuron. There is a latency between the moment the dendrite triggers the dendritic spike and its effect on the soma. All dendritic spikes produce the same stereotypical current pulse effect in the soma. (C) Raster plot of the sequence encoding module in the replay mode, without any dendritic spikes. If dendritic spikes are not allowed, the sequence encoding module produces a replay of the path, but in a much slower time scale. Each transition, in the same way as during encoding, takes between 50 to 100ms. Reverse replays rely crucially on dendritic spikes and cholinergic modulatory effect and do not happen without either. (D) Raster plot of the sequence encoding module in the replay mode, now with dendritic spikes. Dendritic spikes increase the speed of replays by two orders of magnitude, making it in line with what is observed during sharp-wave ripples.

There, the rate of excitation (*red*) and inhibition (*teal*) is shown for varying recurrent excitatory (inhibitory) and compared with the identity (*black*). Formally, to obtain the stable points of activity one has to solve the system of equations: $r_E = F(r_E, r_I)$ and $r_I = G(r_E, r_I)$, where F and G represent the evolution of the rate of excitatory and inhibitory neurons when receiving excitatory rate r_E and inhibitory rate r_I. For the plot, the implicit solution $r_I(x) = G(x, r_I(x))$ is approximated for all x. For the excitatory gain function, the function $F(x, r_I(x))$ (in *red*) is plotted and compared to the identity (in *black*). An analogous procedure is done to plot the inhibitory gain function $G(r_E(x), x)$, where we now define $r_E(x)$ implicitly via the equation $r_E(x) = F(r_E(x), x)$.

Note that the excitatory gain function is below the identy for low rates in Figure 4B but not in Figure 4C. This implies that there is a stable point at 0 Hz while the gating inhibition I_G is active, even when receiving input from the previous bistable unit, but this stable point disappears when I_G is turned inactive. This allows the activity to move forward. On the other hand, in both Figure 4B and 4C, the excitatory gain function is above and then below the identity around the corresponding stable points. This characterizes the stable point as well as the stable region around it.

2.3.2 Encoding mode

The spiking network operates in the encoding mode if the initial excitatory input that activates the first bistable unit does so in an asynchronous manner. If the bistable units exhibit the correct rate dynamics, then the gating and competitive inhibitory mechanisms guarantee that it behaves as intended, again, by a through analysis of the gain functions of excitatory and inhibitory neurons. From the conditions given by the rate dynamics we have: (1) if the gating inhibition I_G is inactive, then the input sent by B_i to B_{i+1} should be enough to activate B_{i+1}; (2) if I_G is active, then B_i remains active; and (3) while I_G is active, B_{i+1} remains silent. Figures 4B, C explain the functioning of the gating inhibitory mechanism. In Figure 4B observe that if I_G is activated then the bistable unit B_i maintains both high and low rate stable points, even when receiving input from the previous bistable unit.

The behavior of the network changes once I_G is inactivated. If bistable unit B_i receives input from the previous bistable unit then the stable point at 0 Hz disappears and only the 50 Hz stable

point remains. This is shown in Figure 4C. Observe that if the gain functions behave as shown in Figure 4B and Figure 4C then the spiking network will satisfy conditions (1), (2) and (3) from above.

We observe a few additional points. Increasing the rate of I_G decreases the gain functions of excitatory and inhibitory neurons. This enlarges the stable region around 0 Hz, but shrinks the stable region around 50 Hz, and also shifting to a slightly smaller rate value. Thus, satisfying the three conditions, corresponds to not shrinking the stable region around 50 Hz by too much in (2) and enlarging the stable region around 0 Hz enough to satisfy (3). This observation also implies that it is not feasible to have the high firing rate stable point at too small firing rates, as satisfying all three conditions is difficult.

Again, from the rate dynamics we see that: once I_G is inactive, and B_{i+1} gets active, the competitive inhibition I_C will spike and guarantee that only B_{i+1} remains active. The competitive inhibition I_C functions here as a coincidence detector of two active bistable units. It remains inactive if only a single bistable unit is active, but once two or more are active, its neurons receive enough excitatory input to spike. Such behavior is a simple consequence of the thresholding of the membrane potential of neurons to produce an action potential. With such a one spike volley, I_C gives strong enough inhibitory input to quickly inactivate B_i, but B_{i+1} recovers and keeps active as it gets excitatory input from B_i and from itself. As soon as the activity B_{i+1} stabilizes, the gating inhibition I_G turns active and prevents activity from going onwards to activate B_{i+2}.

2.3.3 Replay mode

The spiking network is in the replay mode if the first bistable unit is activated in a synchronous manner. This synchronous activation of the neurons in a bistable unit triggers dendritic spikes in neurons in the next bistable unit, which in turn, trigger synchronous spikes at the corresponding neurons and the activity can continue in a synchronous wave, much like in a synfire chain [56]. Such activity travels only forward because the dendrites have a refractory period of 5 ms after transmitting a dendritic spike to the soma.

2.3.4 Reverse replay

The replay mode of the spiking network can produce reverse replays if the last bistable unit is activated synchronously. As in the forward replays, the activity proceeds synchronously through dendritic spikes. Again, it has a single direction of motion, due to the refractory period of the dendritic compartments that produce dendritic spikes. We emphasize that the increased synaptic weights in the replay mode, due to lower ACh levels, are essential if one wants the encoding and reverse replay modes to reliably behave as intended.

2.4 Robustness to noise and parameter variations

We want to point out that the chosen parameters are biologically plausible and do not need to be fine-tuned. To this end, we produce Figure 5, showing that the choice network ensemble sizes and the choice of network weights are not crucial for the spiking network to behave as intended. In Figure 5A and Figure 5B we double the network ensemble sizes, while halving all the weight parameters (alternatively, one could halve the connection probability). The encoding and replay modes function the same way as before. In Figure 5C and Figure 5D we change all the used parameters following the guide of the gain functions and show another set of parameters where the encoding and replay modes behave as intended. We observe that while the conditions of the

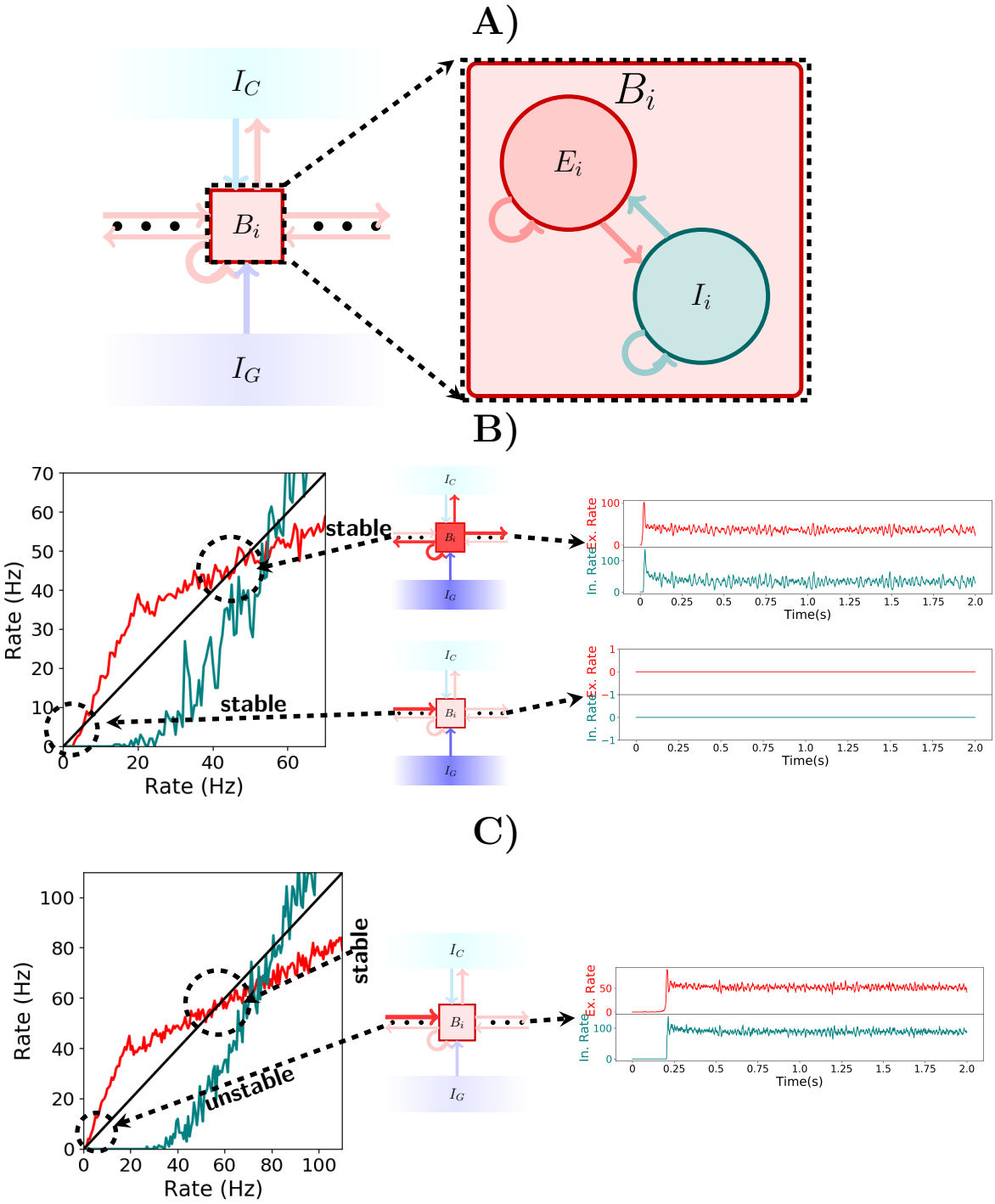
A)
I_C
B_i
I_G
B_i
E_i
I_i
B)
Rate (Hz)
Rate (Hz)
stable
stable
Ex. Rate
In. Rate
Time(s)
C)
Rate (Hz)
Rate (Hz)
stable
unstable
Ex. Rate
In. Rate
Time(s)

Figure 4

Figure 4 *(previous page)*: Spiking network. (A) Illustration of a bistable unit consisting of both an excitatory and an inhibitory population. (B) On the left, the gain function of excitatory (red) and inhibitory(teal) neurons inside a bistable unit B_i is depicted. As shown in the center, if I_G is turned on, then the shape of the gain function produces two stable states, one at 0Hz and another at approximately 50Hz. The stable states are shown on the right. (C) Analogous to (B), but now with I_G turned off. As seen on the left, the gain function shape changes when receiving input from the previous pattern and the stable state at 0Hz ceases to exist. The network always settles for the only stable point around 50Hz, a fact which is shown on the right.

dynamical system imply one cannot take a single parameter and change it significantly, one can change the parameters if a certain set of reasonable conditions is ensured (in other words, one has to respect the coupling among different parameters).

As a final note, we emphasize that the plots in Figure 1 were produced using a gaussian multiplicative noise on each individual weight. It is not crucial for the spiking network that each individual weight is as defined, only that the total average weight inside a particular ensemble or between ensembles is close to the desired values.

3 Discussion

Summary

In this work, we show a model which can store in behavioral time place cell activity traces corresponding to paths run by an animal and produce fast bidirectional replays of these place cell activity traces during sleep and quiet wakefulness, even after a single run of the path. Furthermore, our approach works independently of the geometry of the environment and of particularities of the path taken (such as loops present in it). As observed in the literature, the replays produced by our model have constant speed and are not influenced by the potentially varying speed of the mouse during the run. As the primary conclusion of our model, we predict the existence of a population of sequence cells, dedicated to the task of encoding of sequential activity, which enables the model to properly deal with loops in the path of the mouse. This is an experimentally verifiable hypothesis, as sequence cell firing should be clearly distinguishable from place cell firing, as well as from head direction cells, border cells and so on (time cells [43] could pose a challenge as sequence cells also measure time in a certain sense). Sequence cells enable behavioral time storage of paths traversed and subsequent spontaneous fast replay of place cell activities as observed in rodents during slow-wave sleep and quiet wakefulness. The sequence cells are organized in sequence encoding modules where, crucially, the activity progresses through stereotypical sequences of ensembles. The sequence encoding modules possess two modes of operation one used during encoding and another during replay. The encoding mode relies on a disinhibitory mechanism to control the speed of asynchronous activity progression in the ensembles. The replay mode relies on synchronous activity and resulting dendritic spikes to trigger fast replay of the sequence encoding modules. Lower levels of ACh, leading to higher excitability, allow the sequence encoding modules to be played in reverse - which would also account for the observed reverse replays of place cell activity in rodents. In addition, reverse replays happen mostly after rewards, which in our model, permit the sequence to be played in reverse to find the causes that produced the reward. In particular, a very long sequence encoding module can be used to store multiple paths, by just using the reverse replays to mark

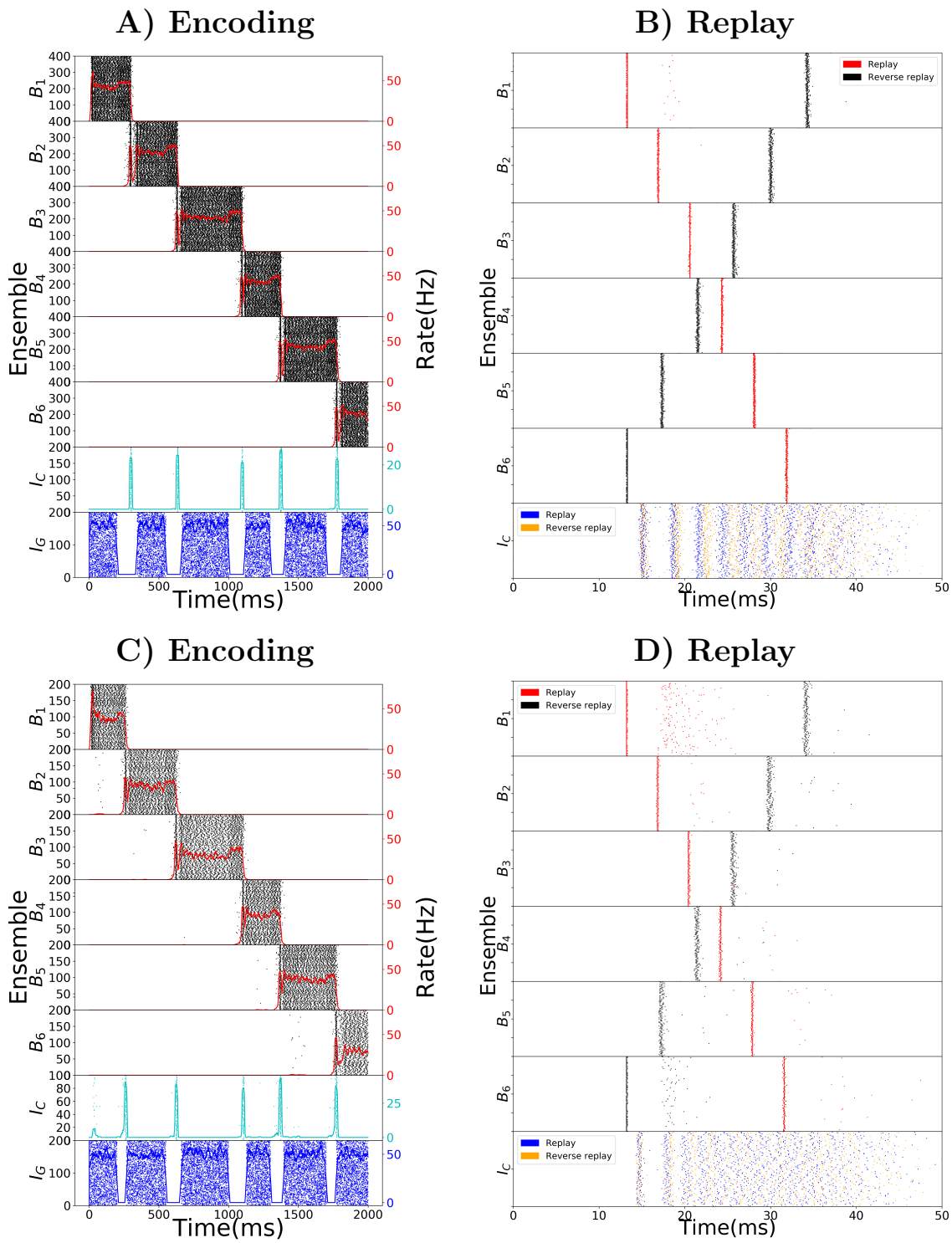
A) Encoding
B) Replay
C) Encoding
D) Replay
Ensemble
Rate(Hz)
Time(ms)
Replay
Reverse replay

Figure 5

Figure 5 *(previous page)*: Robustness to parameter variations. (A) Raster plot of the encoding mode of the sequence encoding module with 6 patterns. The size of ensembles B_i and I_C are doubled, while the connection probability is halved (alternatively, one can half all corresponding weight parameters). This shows that the size of each ensemble is not important for the model to work. (B) Analogous to (A) but now the replay mode is shown. Again each ensemble size is doubled. (C) Raster plot of the encoding mode of the sequence encoding module, with an alternative parameter set (see Table 6). This shows that the choice of parameters we used is not unique. Instead, as long as the conditions on the gain functions are satisfied, there is a large range of weight parameters where the model performs as expected. (D) Raster plot of the replay mode using the alternative parameter set (see Table 6).

the relevant starting and ending positions in the sequence. Effectively, this allows the sequence to be split up in many subsequences, each corresponding to a relevant memory.

In the upcoming subsections, we discuss the bioplausibility of the properties we used, such as how the sequence encoding modules can be formed, the form of inhibitory processing, the dendritic spikes and the different cholinergic environment in movement and quiescence.

Formation of sequence encoding modules

The sequence encoding modules proposed here rely on complex dynamics and a specific connectivity structure. Their structure can either be hardwired, as a product of evolution, or perhaps more likely, emerge as a consequence of the interaction of the many plasticity rules present in the hippocampus. For example, sequences of ensembles forming long synfire chains can spontaneously emerge as a product of spike-timing dependent plasticity (STDP) and axon remodeling [68], or a three factor variant of STDP [69] which is modulated by global population activity [70]. Such long sequences of ensembles form the basis of the sequence encoding modules in here. In addition, in [71], fMRI activity reveals that linearexperimental evidence is presented for attractor dynamics in the hippocampus. Their data shows that linear changes in the environment context induce dynamic, non-linear changes in hippocampal activity patterns. Moreover, [72] present evidence for autoassociative and heteroassociative dynamics in the hippocampus. Densely connected populations representing attractor states (autoassociative dynamics) are sparsely connected among themselves (heteroassociative dynamics), a characteristic which permits sequential processing of information. Their data reveals a fundamental discretization in the memory retrieval processes of the hippocampus, supporting the idea that sequences of attractor states are sparsely connected, as is the case in the sequence encoding modules.

Inhibitory neural processing

Crucial to the proper functioning of the encoding mode of the sequence encoding modules are the two forms of inhibitory neural processing, the gating inhibition and the competitive inhibition. Speed-correlated firing of hippocampal neurons has been reported and is controlled by glutamatergic interneurons in the medial septum [47, 48]. The firing rates of these glutamatergic interneurons are proportional to the speed of locomotion and control the theta oscillations during locomotion, being crucial to the initiation of theta oscillations. These glutamatergic septo-hippocampal projections perform disinhibitory control of the activity in areas CA3 and CA1, which is in line with our proposal of a gating inhibitory mechanism that is switched off during movement, possibly via some disinhibitory mechanism.

Furthermore, a specific type of inhibitory interneurons, called VIP interneurons, are known to have a disinhibitory function and seem to be ubiquitous in the brain [73, 74, 75]. These VIP interneurons perform disinhibitory control in the brain which is activated under specific behavioral conditions [75], a fact which is consistent with our hypothesis that the gating inhibition is switched off when the animal changes its location.

The winner-take-all dynamics implemented using the competitive inhibition are commonplace in the theoretical neuroscience literature [76, 77]. Furthermore, anatomical studies have shown that cortical networks contain essential features which can be implemented via winner-take-all circuits [78, 79].

As the above examples show, there exists a large diversity of inhibitory interneuron subtypes each potentially serving a different purpose [80]. Such diversity of interneuron types and functions is a strong indicator that the simple forms of inhibitory control proposed here can be realized in the brain.

Sharp-wave ripples, dendritic spikes and replays

Previous works [38] also suggest the relation between dendritic spikes, sharp-wave ripples and replays. Our work goes along similar lines, suggesting that replays are a product of synfire chain like behavior, driven by dendritic spikes, of special populations of neurons, that fire in a stereotypical manner, independent of instantial specifics of an animal's movement. Sharp-wave ripples are the most synchronous events reported in the hippocampus [81]. The replay of place cell activities is known to be concurrent with ripple events [31, 20]. Such synchronous events favour the occurrence of dendritic spikes, which, in turn, favour synchronous excitatory activity along a feedforward structure [38, 39].

ACh levels and neuromodulators

It is known that Acetylcholine levels are significantly reduced in slow-wave sleep and quiet wakefulness, in comparison to an awake state [82, 83, 49]. It is further believed that such change in the cholinergic modulation is crucial for the process of acquiring and consolidating new memories [84, 49, 50]. In accordance with this work, [50] proposes that different levels of Acetylcholine during exploration, slow-wave sleep and quiet wakefulness set the appropriate dynamics of the network for encoding and consolidating memories (replays). Lastly, a recent study [85] indicates that replays, in both directions, are more likely to occur after rewards are obtained. In particular, their results suggest that reverse replays could be a mechanism to reinforce experiences that produced rewards. This connects nicely to our work, as replays (and especially reverse replays) in our model rely on higher excitability of the network which could be further provided by increased dopamine effects.

Other models of sequence replay

There are alternative models that achieve partially similar results to the ones reported here. These previous works fail to produce replays which cope with the irregularity of behavior and need specific assumptions about the geometry of the environment or about the trajectory taken. In [36], a short-term synaptic depression mechanism is shown to produce two different regimes of activity of place cell rate dynamics, that can account for replays observed in the literature [15, 20] and preplays [86, 87, 88], at least under the assumption that a map of the environment is stored in the synaptic connections among the place cell rate units. In [37], it is studied how standard plasticity rules [34, 35] shape the patterns of activity of place cell rate units and it is found

that the theta rhythm speeds up encoding of newly explored environments. The mechanism for generating the replays is the same as the one used in [36]. In [40], a spiking network consisting of Hebbian assemblies that are weak and sparsely connected uses pre-existing recurrent connections to quickly amplify weak signals. As in our work, the assemblies are activated like a synfire chain during replays and network states are altered by globally changing neuronal excitability (say, by cholinergic modulation). The authors of [38], in line with our work, propose that sharp-wave ripples and replays are interconnected and that nonlinear dendritic computation, in the form of dendritic sodium spikes, accounts for the observed replays in the rodent hippocampus. As in this work, the dendritic spikes distinguish between an asynchronous state present while the animal is awake and a synchronous activity state, related to sharp-wave ripples, occurring during slow-wave sleep and quiet wakefulness. In [39], dendritic spikes are again used in the generation of replays and preplays of activity. In an hypothesis similar to ours, CA3 possesses innate sequential structure that gives rise to spontaneous firing sequences and can be used to one-shot learn place fields. Still, we note that our sequence encoding modules are the first to account for a compressed representation of place cell activity to produce replays, both forward and reverse, which are independent of the instantial specifics of the animal's movement and environment.

Compressing sequence representations in other contexts

In this work, we restrict sequence processing to a navigation task because the hippocampus is extensively studied in this regard and there are many reported phenomena (sharp-wave ripples, cholinergic modulation, forward and reverse replays, dendritic spikes) which fit well into our framework of sequence encoding modules.

Still, the ability to divide complex tasks into simpler, compounding, sequential subtasks is essential to understand and perform the original more complex task. Identifying these subtasks and their interconnectedness, compressing useful sequences into the most relevant parts and factoring out the non-relevant ones, is an important characteristic if one wants to learn ever more complex behavioral patterns. It is a given that animals perform this form of sequence processing operation on a high-level. In this work, it is further argued that this sequence processing is such an essential operation, that the brain might develop special modules of cells capable of extracting the relevant subparts contained in a more complex task.

4 Materials and Methods

4.1 Reduced rate encoding model

To understand the dynamics of the spiking network, we consider a reduced model where we collapse ensembles into abstract rate units. As before, we denote by $B_1, \ldots, B_\ell$ the ℓ bistable units that form the sequence, by I_C the competitive inhibitory population to all ℓ ensembles and by I_G the gating inhibitory input. The activity of unit X at time t is given by $\lambda_X(t)$ which corresponds to the rate of the ensemble. The units are connected into a network which dictates their interaction. We denote the interaction from unit X to itself by w_X, and the interaction strength from unit Y to X by w_{XY}. The connectivity is as in Figure 2A. We assume that interactions with an inhibitory (excitatory) source negatively (positively) affect the target's rate. Moreover, we assume that the activity $\lambda_{I_G}(t)$ alternates between high and low rate states as depicted in Figure 2B,C. The rate of other units evolves according to the following set of differential equations:

$$\frac{d\lambda_{B_i}(t)}{dt} = f(I_{B_i}(t)) - \lambda_{B_i}(t)$$

for the rate of unit B_i and

$$\frac{d\lambda_{I_C}(t)}{dt} = g(I_{I_{I_C}}(t)) - \lambda_{I_{I_C}}(t)$$

for the rate of unit I_C, where $I_{B_i}(t)$ is:

$$I_{B_i}(t) = w_{B_i}\lambda_{B_i}(t) + w_{B_iB_{i-1}}\lambda_{B_{i-1}}(t) + w_{B_iI_C}\lambda_{I_C}(t) + w_{B_iI_G}\lambda_{I_G}(t)$$

and $I_{I_C}(t)$ is:

$$I_{I_C}(t) = \sum_{i=1}^{\ell} w_{I_CB_i}\lambda_{B_i}(t)$$

and the functions f and g are generally chosen as saturating functions such as the sigmoid function $\frac{e^x}{1+e^x}$. These equations represent how the rate of the populations in the spiking network should evolve, with f and g being gain functions of neurons and $I_{B_i}(t)$ and $I_{I_C}(t)$ being the total input received by the respective neurons. The goal is to set the parameters of the system such that the activity evolves as in Figure 2C.

To produce the dynamics of Figures 2B,C, it is enough to study this rate model with two bistable units B_i and B_{i+1}, with the additional constraint that weights from and to B_i are equal to those from and to B_{i+1}. This allows for a simple extension to ℓ bistable units, as the symmetry of the weights guarantees that the system will have the same rate dynamics independent of which bistable unit is currently active. In particular, with only two bistable units, it is possible, under the assumption that f and g are piecewise linear, to write a simple dynamical system of equations that can be fully solved and understood.

Moreover, it is crucial that f is chosen to guarantee bistable rate dynamics of each B_i, that is, specifically that close to zero or negative input produces silent (zero rate) responses and that large enough inputs produce a maximal rate response. In addition, from g it is required that it guarantees the behavior we expect from I_C, namely, that it serves as a detector for two bistable units being active at the same time, producing maximal response if it receives input from two bistable units close to the maximal response, and being silent if it receives not much more than what a single maximally active bistable unit can produce.

Given this, one can state simple requirements that are essential: (1) that the system is at a stable point while B_1 is at its maximal rate, B_2 silent and I_G is at the high rate state. (2) that B_1 can activate B_2 to its maximal rate once I_G is at the low rate state; (3) that the rate of I_C increases when both bistable units are jointly active; (4) I_C being active is strong enough to turn silent both B_1 and B_2; (5) the speed of the inhibitory I_C dynamics is faster than that of B_1 and B_2, which can force B_1 below the point where it can reactivate itself, while B_2 remains above said point. In particular, the speed of inhibitory I_C dynamics is crucial to guarantee that the rate system can produce the desired rate dynamics with symmetric weights.

These requirements of the rate-based system, therefore, imply that one of three possible outcomes can happen, where only the third is desired: (1) B_i and B_{i+1} turn both inactive; (2) the rates of B_i, B_{i+1} and I_C oscillate; (3) B_i turns inactive, but B_{i+1} stays active, driven by activity in B_i and by its own dynamics.

Table 1: Summary of parameters for the rate model.

Symbol	Description
w_X	synaptic strength between neurons in X
w_{XY}	synaptic strength from neuron in Y to X
$\lambda_X(t)$	activity of unit X at time t
$I_X(t)$	total input received by unit X
$f(I)$	gain function of the ℓ bistable units B_i
$g(I)$	gain function of inhibitory I_C

Overview of parameters - rate model

Table 1, we summarize the notation and parameters used in the rate reduced model.

4.2 Spiking network

4.2.1 Neuron models

In the spiking version of the model each ensemble unit is composed of an excitatory (E_x) population with N^E units and an inhibitory (I_x) population with N^I units where the lower-case subscript x corresponds to the index of the pattern. We follow the convention of denoting the populations by superscript and the neuron index by subscripts. The membrane potential dynamics of neuron i in population X follow:

$$\begin{aligned}\frac{d}{dt}V_i^X(t) =& \frac{1}{\tau^X}\left(E_L^X - V_i^X(t) + \Delta_T^X \exp\left(\frac{V_i^X(t) - V_{T,i}^X(t)}{\Delta_T^X}\right)\right) \\ &+ \frac{g_i^{XE}(t)}{C}(E^E - V_i^X(t)) + \frac{g_i^{XI}(t)}{C} - \frac{w_i^X(t)}{C}.\end{aligned}$$

The parameter values are summarized in Table 2 and the dynamics are consistent with [89, 52]. The main difference between the excitatory and inhibitory units is that the excitatory neurons have an adaptation current and an adaptive threshold [90, 91] whereas the inhibitory neurons are non-adapting. The adaptive threshold follows:

$$\frac{d}{dt}V_{T,i}^{E_x} = \frac{1}{\tau_T}\left(V_T - V_{T,i}^{E_x}(t)\right). \tag{1}$$

We record a spike when the voltage exceeds $20mV$ and we reset it to and hold it at V_{re} for the refractory period duration τ_{abs}. For an adaptive threshold we set it to $V_T + A_T$ after a spike. The adaptation current for a neuron in population E_x follows:

$$\frac{d}{dt}w_i^{E_x}(t) = \frac{1}{\tau_w}\left(a_w\left(V_i^{E_x}(t) - E_L^{E_x}\right) - w_i^{E_x}(t)\right) \tag{2}$$

and it is increased by b_w when neuron i spikes.

4.2.2 Synapse dynamics

Connection probability between population X and Y is given by p^{XY} and the strength of a connection between unit $i \in X$ and unit $j \in Y$ is given by w_{ij}^{XY}. The total conductance of

neuron i in population X from a source of type Y (excitatory or inhibitory) follows:

$$g_i^{XY}(t) = F^Y(t) * \left(w_{\text{ext}}^{XY} s_{i,\text{ext}}^{XY}(t) + \sum_{Y_k \in Y} \sum_j w_{ij}^{XY_k} s_j^{Y_k}(t) \right), \tag{3}$$

where $F^Y(t) = \frac{1}{\tau_d^Y - \tau_r^Y}\left(e^{-t/\tau_d^Y} - e^{-t/\tau_r^Y}\right)$ is the synaptic kernel for input from neurons of type Y, Y_k corresponds to subpopulations of type Y, $*$ is the convolution operator and $s_j^{Y_k}(t) = \sum_{\ell=1}^{n} \delta(t - t_{i,\ell}^{Y_k})$ denotes the spike train of neuron j in population Y_k. Additionally, each neuron receives external input given by the spike train $s_{i,\text{ext}}^{XY}(t)$ which follows a homogeneous Poisson process with rate r_{ext}^{XY} and weight w_{ext}^{XY} for neurons in population X where Y can either be an excitatory (E) or an inhibitory (I) source. The resolution of the simulation is 0.1 ms and the coupling parameters can be found in Table 3.

4.2.3 Dendritic spikes

Dendritic spikes are triggered by excitatory spikes arriving in a short time span at a particular position in the dendrite of a neuron. We incorporate them by setting the synaptic conductance of the afferent input to produce a stereotypical current pulse, using parameters observed in single-neuron experiments [57, 58, 59, 60] and similar to the one used in recent spiking network models [61, 62, 38]. Whenever the excitatory input to a (dendritic branch of) a neuron changes the conductance of the neuron by a threshold θ_{dspike} in a time window of 2 ms, a dendritic spike is initiated. This produces a stereotypical current pulse at the soma whose effect is triggered with a time lag of τ_{DS} after the dendritic threshold is crossed. This time lag is on the same order as the one observed in single neuron experiments. The stereotypical current pulse, like that of [38], is described by:

$$I_{ds} = \Theta(t - \tau^{DS}) \left[-A \exp^{\left(-\frac{t-\tau^{DS}}{\tau^{ds,1}}\right)} + B \exp^{\left(-\frac{t-\tau^{DS}}{\tau^{ds,2}}\right)} - C \exp^{\left(-\frac{t-\tau^{DS}}{\tau^{ds,3}}\right)} \right]$$

where the factors A, B, C and the decay time constants $\tau^{ds,1}$, $\tau^{ds,2}$, $\tau^{ds,3}$ are chosen so that the depolarizing effect on the soma fits experimental data [57, 58, 59, 60], and whose values are shown in Table 4. Moreover, we add a refractory period $t^{ref,ds} = 5$ ms, as in [61, 62, 38], to these dendritic branches after the stereotypical current pulse has influenced the soma, in accordance to the saturating effect of somatic depolarization of dendritic spikes reported in the literature [57].

4.2.4 Cholinergic modulation

In accordance with [84, 49, 50], we use the fact that, during exploration, high levels of cholinergic modulation are present and the excitatory feedback is thus in part suppressed; during sleep and quiet wakefulness, the ACh levels drop and this suppression is reduced, thus leading to generally stronger synaptic weights. We use a simple 2.5 factor to increase the strength of excitatory synapses during the replay mode in comparison with the encoding mode. Though not too much data is available on the cholinergic effect in vivo, this factor is in line with the one obtained from hippocampal slices of areas CA3 and CA1 in rats [92, 66].

4.2.5 Hebbian plasticity from sequence to place cells

To connect a bistable unit in the sequence encoding module with the corresponding population of place cells, we use a Hebbian like plasticity mechanism. Initially, all synapses from sequence to place cells are silent, and they are potentiated and turned active if the corresponding pre and post cells fire at high rates in a short period. The exact implementation was done by a voltage-based STDP plasticity rule [89] which tends to increase synaptic weight if both pre and post neurons have a high firing rate. As the process of activating a silent synapse is equivalent to LTP [93, 94], we speed up the dynamics to make it consistent with the timescale of LTP. In accordance with [89, 52], the dynamics of the synaptic strength w_{ij} from sequence cell j to place cell i are given as:

$$\frac{d}{dt}w_{ij}(t) = -A_{LTD}s_j(t)R\left(u_i(t) - \theta_{LTD}\right) + A_{LTP}x_j(t)R\left(V_i(t) - \theta_{LTP}\right)\left(v_i(t) - \theta_{LTP}\right)$$

where $R(x)$ is a linear-rectifying function, that is, $R(x) = 0$ if $x \leq 0$ and $R(x) = x$ otherwise; u_i and v_i represent the membrane voltage V_i low-pass filtered with time constants τ_u and τ_v respectively; and x_j represents the spike train s_j low-pass filtered with time constant τ_x. The constants $A_{LTD}, A_{LTP}, \theta_{LTD}, \theta_{LTP}$, τ_u, τ_v and τ_x are given in Table 5 and are the same as [52], with the exception of A_{LTP}, which is increased to speed up the dynamics and bring the timescale of activating a synapse into the hundred milliseconds range. Furthermore, the maximum value of w_{ij} is $5pF$.

4.3 Overview of parameters

Here we summarize the parameters of the spiking neural network simulation of exponential integrate-and-fire neurons. Table 2 and Table 3 contain the parameters regarding the membrane potential dynamics of a neuron, and the parameters regarding the neuronal coupling, respectively. Table 4 contains the dendritic spikes parameters that were used, and Table 5 the Hebbian plasticity ones.

For Figure 1, we use a multiplicative gaussian noise $\mathcal{N}(1, 0.2)$ for each individual synaptic weight (shown in Table 3) in the spiking network. For Figure 5C,D, we use a different set of synaptic weights which we show in Table 6.

5 Supplementary video

We produced a video animation to enhance the comprehension of what the model achieves. It can be found at: www.dropbox.com/s/o8ryq5lb0kd8oiu/sequence_replay_video.mp4?dl=0.

References

[1] Scoville WB, Milner B. Loss of recent memory after bilateral hippocampal lesions. Journal of neurology, neurosurgery, and psychiatry. 1957;20(1):11.

[2] O'keefe J, Nadel L. The hippocampus as a cognitive map. Oxford: Clarendon Press; 1978.

[3] Squire LR, Zola-Morgan S. The medial temporal lobe memory system. Science. 1991;253(5026):1380.

Table 2: Summary of parameters for membrane dynamics.

Symbol	**Description**	**Value**
τ_{E_x}	E_x neuron resting membrane time constant	20 ms
τ_{I_x}	I_x neuron resting membrane time constant	20 ms
$E_L^{E_x}$	E_x neuron resting potential	-70 mV
$E_L^{I_x}$	I_x neuron resting potential	-62 mV
$\Delta_T^{E_x}$	E_x neuron EIF slope factor	2 mV
C	Membrane capacitance	300 pF
E^{E_x}	E_x neuron reversal potential	0 mV
E^{I_x}	I_x neuron reversal potential	-75 mV
V_T	Threshold potential	-52 mV
A_T	Post spike threshold potential increase	10 mV
τ_T	Adaptive threshold timescale	30 ms
V_{re}	Reset potential	-60 mV
τ_{abs}	Absolute refractory period	1 ms
a_w	Subthreshold adaptation	4 nS
b_w	Spike-triggered adaptation	0.8 pA
τ_w	Spike-triggered adaptation timescale	150 ms

[4] Eichenbaum H, Cohen NJ. From conditioning to conscious recollection: Memory systems of the brain. 35. Oxford University Press on Demand; 2004.

[5] Davachi L, Burgess N. Editorial overview: Memory in time and space. Elsevier; 2017.

[6] Squire LR. The neuropsychology of human memory. Annual review of neuroscience. 1982;5(1):241–273.

[7] Eichenbaum H. Memory, amnesia, and the hippocampal system. MIT press; 1993.

[8] Rudy JW, Sutherland RJ. Configural association theory and the hippocampal formation: an appraisal and reconfiguration. Hippocampus. 1995;5(5):375–389.

[9] Vanderwolf CH. Hippocampal electrical activity and voluntary movement in the rat. Electroencephalography and clinical neurophysiology. 1969;26(4):407–418.

[10] Buzsáki G. Theta oscillations in the hippocampus. Neuron. 2002;33(3):325–340.

[11] Hasselmo ME, Bodelón C, Wyble BP. A proposed function for hippocampal theta rhythm: separate phases of encoding and retrieval enhance reversal of prior learning. Neural computation. 2002;14(4):793–817.

[12] Buzsáki G. Hippocampal sharp waves: their origin and significance. Brain research. 1986;398(2):242–252.

[13] Buzsáki G. Two-stage model of memory trace formation: a role for "noisy" brain states. Neuroscience. 1989;31(3):551–570.

[14] Buzsáki G. Hippocampal sharp wave-ripple: A cognitive biomarker for episodic memory and planning. Hippocampus. 2015;25(10):1073–1188.

Table 3: Summary of parameters for neuronal coupling.

Symbol	Description	Value
N^{E_x}	Number of neurons in population E_x	200
N^{I_x}	Number of neurons in population I_x	100
N^{I_C}	Number of neurons in population I_C	100
N^{I_G}	Number of neurons in population I_G	100
p	Connection probability	0.2
τ_r^E	Rise time for excitatory synapses	1 ms
τ_d^E	Decay time for excitatory synapses	6 ms
τ_r^I	Rise time for inhibitory synapses	0.5 ms
τ_d^I	Decay time for inhibitory synapses	2 ms
$r_{\text{ext}}^{E_xE}$	Rate of external excitatory input	1.0 kHz
$r_{\text{ext}}^{E_xI}$	Rate of external inhibitory input	1.0 kHz
$r_{\text{ext}}^{I_xE}$	Rate of external excitatory input	1.0 kHz
$r_{\text{ext}}^{I_xI}$	Rate of external inhibitory input	1.0 kHz
r^{XI_G}	Rate of I_G input to X	0.05 kHz
w^{XI_G}	Weight of I_G input to X	2.5 pF
$w^{E_xE_x}$	Excitatory to excitatory strength	10 pF
$w^{E_xI_x}$	Inhibitory to excitatory strength	10 pF
$w^{I_xE_x}$	Excitatory to inhibitory strength	4 pF
$w^{I_xI_x}$	Excitatory to inhibitory strength	3 pF
$w^{E_{x+1}E_x}$	Forward afferent strength	1.6 pF
$w^{E_xE_{x+1}}$	Backward afferent strength	0.8 pF
$w^{I_CE_x}$	Excitatory to competitive inhibitory strength	1.5 pF
$w^{E_xI_C}$	Competitive inhibitory to excitatory strength	12 pF
$w_{\text{ext}}^{E_xE}$	External excitation to excitation strength	2 pF
$w_{\text{ext}}^{I_xE}$	External excitation to inhibition strength	0 pF
$w_{\text{ext}}^{E_xI}$	External inhibition to excitation strength	0 pF
$w_{\text{ext}}^{I_xI}$	External inhibition to inhibition strength	4 pF

Table 4: Summary of parameters for dendritic spikes.

Symbol	Description	Value
A	dendritic input pulse constant	55 nA
B	dendritic input pulse constant	64 nA
C	dendritic input pulse constant	9 nA
τ^{DS}	dendritic spikes latency	2.7 ms
$\tau^{ds,1}$	Decay time for dendritic input pulse curve	0.2 ms
$\tau^{ds,2}$	Decay time for dendritic input pulse curve	0.3 ms
$\tau^{ds,3}$	Decay time for dendritic input pulse curve	0.7 ms
θ_{dspike}	Conductance slope threshold for NMDA spikes	6.0 pF

Table 5: Summary of plasticity parameters.

Symbol	**Description**	**Value**
A_{LTD}	LTD strength	$0.0008pAmV^{-1}$
A_{LTP}	LTP strength	$0.07pAmV^{-1}$
θ_{LTD}	threshold to recruit LTD	-70 mV
θ_{LTP}	threshold to recruit LTP	-49 mV
τ_u	time constant of low-pass filtered voltage (LTD)	10 ms
τ_v	time constant of low-pass filtered voltage (LTP)	7 ms
τ_x	time constant of low-pass filtered spike-train	15 ms

Table 6: Summary of alternative parameters for neuronal coupling.

Symbol	**Description**	**Value**
r^{XI_G}	Rate of I_G input to X	0.05 kHz
w^{XI_G}	Weight of I_G input to X	1.5 pF
$w^{E_xE_x}$	Excitatory to excitatory strength	8 pF
$w^{E_xI_x}$	Inhibitory to excitatory strength	6 pF
$w^{I_xE_x}$	Excitatory to inhibitory strength	4 pF
$w^{I_xI_x}$	Excitatory to inhibitory strength	2 pF
$w^{E_{x+1}E_x}$	Forward afferent strength	1.3 pF
$w^{E_xE_{x+1}}$	Backward afferent strength	0.65 pF
$w^{I_CE_x}$	Excitatory to competitive inhibitory strength	1.8 pF
$w^{E_xI_C}$	Competitive inhibitory to excitatory strength	5.5 pF
$w_{\text{ext}}^{E_xE}$	External excitation to excitation strength	3 pF
$w_{\text{ext}}^{I_xE}$	External excitation to inhibition strength	0 pF
$w_{\text{ext}}^{E_xI}$	External inhibition to excitation strength	0 pF
$w_{\text{ext}}^{I_xI}$	External inhibition to inhibition strength	3 pF

[15] Wilson MA, McNaughton BL. Reactivation of hippocampal ensemble memories during sleep. Science. 1994;265(5172):676–679.

[16] Diekelmann S, Born J. Slow-wave sleep takes the leading role in memory reorganization. Nature Reviews Neuroscience. 2010;11(3):218.

[17] Girardeau G, Zugaro M. Hippocampal ripples and memory consolidation. Current opinion in neurobiology. 2011;21(3):452–459.

[18] Middleton SJ, Kneller EM, Chen S, Ogiwara I, Montal M, Yamakawa K, et al. Altered hippocampal replay is associated with memory impairment in mice heterozygous for the Scn2a gene. Nature Neuroscience. 2018;.

[19] Kitamura T, Ogawa SK, Roy DS, Okuyama T, Morrissey MD, Smith LM, et al. Engrams and circuits crucial for systems consolidation of a memory. Science. 2017;356(6333):73–78.

[20] Lee AK, Wilson MA. Memory of sequential experience in the hippocampus during slow wave sleep. Neuron. 2002;36(6):1183–1194.

[21] Carr MF, Jadhav SP, Frank LM. Hippocampal replay in the awake state: a potential substrate for memory consolidation and retrieval. Nature neuroscience. 2011;14(2):147–153.

[22] O'Keefe J. Place units in the hippocampus of the freely moving rat. Experimental neurology. 1976;51(1):78–109.

[23] Morris R, Garrud P, Rawlins Ja, O'Keefe J. Place navigation impaired in rats with hippocampal lesions. Nature. 1982;297(5868):681–683.

[24] O'Keefe J, Dostrovsky J. The hippocampus as a spatial map. Preliminary evidence from unit activity in the freely-moving rat. Brain research. 1971;34(1):171–175.

[25] Harvey CD, Collman F, Dombeck DA, Tank DW. Intracellular dynamics of hippocampal place cells during virtual navigation. Nature. 2009;461(7266):941.

[26] Foster DJ, Wilson MA. Reverse replay of behavioural sequences in hippocampal place cells during the awake state. Nature. 2006;440(7084):680.

[27] Karlsson MP, Frank LM. Awake replay of remote experiences in the hippocampus. Nature neuroscience. 2009;12(7):913–918.

[28] Yamamoto J, Tonegawa S. Direct medial entorhinal cortex input to hippocampal CA1 is crucial for extended quiet awake replay. Neuron. 2017;96(1):217–227.

[29] Foster DJ. Replay comes of age. Annual review of neuroscience. 2017;40:581–602.

[30] Pfeiffer BE. The content of hippocampal replay. Hippocampus. 2017;.

[31] Nádasdy Z, Hirase H, Czurkó A, Csicsvari J, Buzsáki G. Replay and time compression of recurring spike sequences in the hippocampus. Journal of Neuroscience. 1999;19(21):9497–9507.

[32] Geisler C, Robbe D, Zugaro M, Sirota A, Buzsáki G. Hippocampal place cell assemblies are speed-controlled oscillators. Proceedings of the National Academy of Sciences. 2007;104(19):8149–8154.

[33] Davidson TJ, Kloosterman F, Wilson MA. Hippocampal replay of extended experience. Neuron. 2009;63(4):497–507.

[34] Markram H, Lübke J, Frotscher M, Sakmann B. Regulation of synaptic efficacy by coincidence of postsynaptic APs and EPSPs. Science. 1997;275(5297):213–215.

[35] Bi Gq, Poo Mm. Synaptic modifications in cultured hippocampal neurons: dependence on spike timing, synaptic strength, and postsynaptic cell type. Journal of neuroscience. 1998;18(24):10464–10472.

[36] Romani S, Tsodyks M. Short-term plasticity based network model of place cells dynamics. Hippocampus. 2015;25(1):94–105.

[37] Theodoni P, Rovira B, Roxin A. A Model Of Plasticity-Dependent Network Activity In Rodent Hippocampus During Exploration Of Novel Environments. bioRxiv. 2017;p. 118489.

[38] Jahnke S, Timme M, Memmesheimer RM. A unified dynamic model for learning, replay, and sharp-wave/ripples. Journal of Neuroscience. 2015;35(49):16236–16258.

[39] Haga T, Fukai T. Dendritic processing of spontaneous neuronal sequences for one-shot learning. bioRxiv. 2017;p. 165613.

[40] Chenkov N, Sprekeler H, Kempter R. Memory replay in balanced recurrent networks. PLoS computational biology. 2017;13(1):e1005359.

[41] Wu X, Foster DJ. Hippocampal replay captures the unique topological structure of a novel environment. Journal of Neuroscience. 2014;34(19):6459–6469.

[42] Grieves RM, Wood ER, Dudchenko PA. Place cells on a maze encode routes rather than destinations. Elife. 2016;5:e15986.

[43] Eichenbaum H. Time cells in the hippocampus: a new dimension for mapping memories. Nature Reviews Neuroscience. 2014;15(11):732.

[44] Bilkey DK, Schwartzkroin PA. Variation in electrophysiology and morphology of hippocampal CA3 pyramidal cells. Brain research. 1990;514(1):77–83.

[45] Buckmaster PS, Amaral DG. Intracellular recording and labeling of mossy cells and proximal CA3 pyramidal cells in macaque monkeys. Journal of Comparative Neurology. 2001;430(2):264–281.

[46] Soltesz I, Losonczy A. CA1 pyramidal cell diversity enabling parallel information processing in the hippocampus. Nature Neuroscience. 2018;21(4):484–493.

[47] Fuhrmann F, Justus D, Sosulina L, Kaneko H, Beutel T, Friedrichs D, et al. Locomotion, theta oscillations, and the speed-correlated firing of hippocampal neurons are controlled by a medial septal glutamatergic circuit. Neuron. 2015;86(5):1253–1264.

[48] Justus D, Dalügge D, Bothe S, Fuhrmann F, Hannes C, Kaneko H, et al. Glutamatergic synaptic integration of locomotion speed via septoentorhinal projections. Nature neuroscience. 2017;20(1):16–19.

[49] Hasselmo ME. Neuromodulation: acetylcholine and memory consolidation. Trends in cognitive sciences. 1999;3(9):351–359.

[50] Hasselmo ME. The role of acetylcholine in learning and memory. Current opinion in neurobiology. 2006;16(6):710–715.

[51] Vandecasteele M, Varga V, Berényi A, Papp E, Barthó P, Venance L, et al. Optogenetic activation of septal cholinergic neurons suppresses sharp wave ripples and enhances theta oscillations in the hippocampus. Proceedings of the National Academy of Sciences. 2014;111(37):13535–13540.

[52] Litwin-Kumar A, Doiron B. Formation and maintenance of neuronal assemblies through synaptic plasticity. Nature Communications. 2014 Nov;5:5319. Available from: `http://www.nature.com/doifinder/10.1038/ncomms6319`.

[53] Zenke F, Agnes EJ, Gerstner W. Diverse synaptic plasticity mechanisms orchestrated to form and retrieve memories in spiking neural networks. Nature communications. 2015;6:6922.

[54] Van Vreeswijk C, Sompolinsky H. Chaos in neuronal networks with balanced excitatory and inhibitory activity. Science. 1996;274(5293):1724–1726.

[55] Renart A, De La Rocha J, Bartho P, Hollender L, Parga N, Reyes A, et al. The asynchronous state in cortical circuits. science. 2010;327(5965):587–590.

[56] Abeles M. Local Cortical Circuits. Springer, Berlin; 1982.

[57] Ariav G, Polsky A, Schiller J. Submillisecond precision of the input-output transformation function mediated by fast sodium dendritic spikes in basal dendrites of CA1 pyramidal neurons. Journal of Neuroscience. 2003;23(21):7750–7758.

[58] Gasparini S, Migliore M, Magee JC. On the initiation and propagation of dendritic spikes in CA1 pyramidal neurons. Journal of Neuroscience. 2004;24(49):11046–11056.

[59] Polsky A, Mel BW, Schiller J. Computational subunits in thin dendrites of pyramidal cells. Nature neuroscience. 2004;7(6):621.

[60] Gasparini S, Magee JC. State-dependent dendritic computation in hippocampal CA1 pyramidal neurons. Journal of Neuroscience. 2006;26(7):2088–2100.

[61] Memmesheimer RM. Quantitative prediction of intermittent high-frequency oscillations in neural networks with supralinear dendritic interactions. Proceedings of the National Academy of Sciences. 2010;107(24):11092–11097.

[62] Jahnke S, Timme M, Memmesheimer RM. Guiding synchrony through random networks. Physical Review X. 2012;2(4):041016.

[63] Buzsaki G. Rhythms of the Brain. Oxford University Press; 2006.

[64] Diba K, Buzsáki G. Forward and reverse hippocampal place-cell sequences during ripples. Nature neuroscience. 2007;10(10):1241.

[65] Louie K, Wilson MA. Temporally structured replay of awake hippocampal ensemble activity during rapid eye movement sleep. Neuron. 2001;29(1):145–156.

[66] Hasselmo ME, Schnell E, Barkai E. Dynamics of learning and recall at excitatory recurrent synapses and cholinergic modulation in rat hippocampal region CA3. Journal of Neuroscience. 1995;15(7):5249–5262.

[67] Gerstner W, Kistler WM, Naud R, Paninski L. Neuronal dynamics: From single neurons to networks and models of cognition. Cambridge University Press; 2014.

[68] Jun JK, Jin DZ. Development of neural circuitry for precise temporal sequences through spontaneous activity, axon remodeling, and synaptic plasticity. PLoS One. 2007;2(8):e723.

[69] Frémaux N, Gerstner W. Neuromodulated spike-timing-dependent plasticity, and theory of three-factor learning rules. Frontiers in neural circuits. 2015;9.

[70] Weissenberger F, Meier F, Lengler J, Einarsson H, Steger A. Long Synfire Chains Emerge by Spike-Timing Dependent Plasticity Modulated by Population Activity. International journal of neural systems. 2017;27(08):1750044.

[71] Steemers B, Vicente-Grabovetsky A, Barry C, Smulders P, Schröder TN, Burgess N, et al. Hippocampal attractor dynamics predict memory-based decision making. Current Biology. 2016;26(13):1750–1757.

[72] Pfeiffer BE, Foster DJ. Autoassociative dynamics in the generation of sequences of hippocampal place cells. Science. 2015;349(6244):180–183.

[73] Letzkus JJ, Wolff SB, Meyer EM, Tovote P, Courtin J, Herry C, et al. A disinhibitory microcircuit for associative fear learning in the auditory cortex. Nature. 2011;480(7377):331.

[74] Jiang X, Wang G, Lee AJ, Stornetta RL, Zhu JJ. The organization of two new cortical interneuronal circuits. Nature neuroscience. 2013;16(2):210–218.

[75] Pi HJ, Hangya B, Kvitsiani D, Sanders JI, Huang ZJ, Kepecs A. Cortical interneurons that specialize in disinhibitory control. Nature. 2013;503(7477):521.

[76] Maass W. On the computational power of winner-take-all. Neural computation. 2000;12(11):2519–2535.

[77] Binas J, Rutishauser U, Indiveri G, Pfeiffer M. Learning and stabilization of winner-take-all dynamics through interacting excitatory and inhibitory plasticity. Frontiers in computational neuroscience. 2014;8:68.

[78] Douglas RJ, Martin KA. Neuronal circuits of the neocortex. Annu Rev Neurosci. 2004;27:419–451.

[79] Carandini M, Heeger DJ. Normalization as a canonical neural computation. Nature Reviews Neuroscience. 2012;13(1):51.

[80] Petilla Interneuron Nomenclature Group, et al. Petilla terminology: nomenclature of features of GABAergic interneurons of the cerebral cortex. Nature reviews Neuroscience. 2008;9(7):557.

[81] Ylinen A, Bragin A, Nádasdy Z, Jandó G, Szabo I, Sik A, et al. Sharp wave-associated high-frequency oscillation (200 Hz) in the intact hippocampus: network and intracellular mechanisms. Journal of Neuroscience. 1995;15(1):30–46.

[82] Kametani H, Kawamura H. Alterations in acetylcholine release in the rat hippocampus during sleep-wakefulness detected by intracerebral dialysis. Life sciences. 1990;47(5):421–426.

[83] Marrosu F, Portas C, Mascia MS, Casu MA, Fà M, Giagheddu M, et al. Microdialysis measurement of cortical and hippocampal acetylcholine release during sleep-wake cycle in freely moving cats. Brain research. 1995;671(2):329–332.

[84] Hasselmo ME, Bower JM. Acetylcholine and memory. Trends in neurosciences. 1993;16(6):218–222.

[85] Singer AC, Frank LM. Rewarded outcomes enhance reactivation of experience in the hippocampus. Neuron. 2009;64(6):910–921.

[86] Dragoi G, Tonegawa S. Preplay of future place cell sequences by hippocampal cellular assemblies. Nature. 2011;469(7330):397.

[87] Ólafsdóttir HF, Barry C, Saleem AB, Hassabis D, Spiers HJ. Hippocampal place cells construct reward related sequences through unexplored space. Elife. 2015;4:e06063.

[88] Grosmark AD, Buzsáki G. Diversity in neural firing dynamics supports both rigid and learned hippocampal sequences. Science. 2016;351(6280):1440–1443.

[89] Clopath C, Büsing L, Vasilaki E, Gerstner W. Connectivity reflects coding: a model of voltage-based STDP with homeostasis. Nature Neuroscience. 2010 Mar;13(3):344–352. Available from: `http://www.nature.com/neuro/journal/v13/n3/abs/nn.2479.html`.

[90] Brette R, Gerstner W. Adaptive Exponential Integrate-and-Fire Model as an Effective Description of Neuronal Activity. Journal of Neurophysiology. 2005 Nov;94(5):3637–3642. Available from: `http://jn.physiology.org/content/94/5/3637`.

[91] Badel L, Lefort S, Brette R, Petersen CCH, Gerstner W, Richardson MJE. Dynamic I-V Curves Are Reliable Predictors of Naturalistic Pyramidal-Neuron Voltage Traces. Journal of Neurophysiology. 2008 Feb;99(2):656–666. Available from: `http://jn.physiology.org/content/99/2/656`.

[92] Hasselmo ME, Schnell E. Laminar selectivity of the cholinergic suppression of synaptic transmission in rat hippocampal region CA1: computational modeling and brain slice physiology. Journal of Neuroscience. 1994;14(6):3898–3914.

[93] Isaac JT, Nicoll RA, Malenka RC. Evidence for silent synapses: implications for the expression of LTP. Neuron. 1995;15(2):427–434.

[94] Kerchner GA, Nicoll RA. Silent synapses and the emergence of a postsynaptic mechanism for LTP. Nature reviews Neuroscience. 2008;9(11):813.